

JENA-90049

DEPARTMENT OF THE INTERIOR
U.S. GEOLOGICAL SURVEY

**High-Resolution Sidescan-Sonar Imagery Of The Manchas
Interiores - Manchas Exteriores Coral Reef Complex,
Mayaguez, Puerto Rico**

{CRUISE REPORT: JA-90-3}

by

W.C. Schwab¹, R.M.T. Webb², W.W. Danforth¹, T.F. O'Brien¹, and B.J.
Irwin¹

Open-File Report Report 91-436

This report is preliminary and has not been reviewed for conformity with the U.S. Geological Survey editorial standards or with the North American Stratigraphic Code. Any use of trade, product, or firm names is for descriptive purposes only and does not imply endorsement by the U.S. Government.

¹U.S. Geological Survey, Woods Hole, MA

²U.S. Geological Survey, San Juan, Puerto Rico

SHIP NAME: Jean A
CRUISE # AND LEG: JA-90-3
PROJECT # AND NAME: 9470-04056, Anasco River (WRD)
FUNDING AGENCY: USGS, WRD, San Juan
CONTRACT: N/A
AREA OF OPERATION: Mayaguez Bay, Puerto Rico
DATES AND PORTS OF CALL: 12-7-92 to 12-15-92; Day trips out of Mayaguez
CHIEF SCIENTIST(S): William C. Schwab & Richard Webb
SHIP'S CAPTAIN: Richy Paul-Rodriguez
SCIENTIFIC PARTY:

William Schwab - USGS
Richard Webb - USGS
William Danforth - USGS
Thomas O'Brien - USGS
Barry Irwin - USGS
Rafael Rodriguez - USGS

PURPOSE OF CRUISE: High-resolution mapping of a coral reef complex and surrounding area (see attached Open File Report).

NAVIGATION TECHNIQUES: Mini-Ranger (shore based)

SCIENTIFIC EQUIPMENT: Klein Side-scan sonar, Geo-Pulse, 3.5 kHz profiler, shipek sampler.

TABULATED INFORMATION: see the Open-File. If you want it, it is there.

PAGE-SIZE TRACKLINE MAP: Due to the close spacing of this type of survey, a page-size trackline map is useless....also difficult to create. See Plate 2 of the Open File.

INTRODUCTION

The Puerto Rico Aqueducts and Sewer Authority is presently seeking a waiver for secondary treatment of sewage from the Mayaguez regional water treatment plant. The U.S. Environmental Protection Agency has tentatively denied the waiver. Their primary concern has been the potential impact of the outfall on the surrounding marine ecosystem which includes a live coral reef complex, the Manchas Interiores and Manchas Exteriores (Fig. 1). The Rio (River) Grande de Anasco also empties into this study area, carrying a significant load of suspended sediment and contaminants that may further stress the marine community. In order to assess adequately the relative significance of the different sources of reef stress, a program was initiated to monitor the sediment and water-quality characteristics of the Rio Grande de Anasco in addition to sampling of effluent, ocean water, and sediment in the vicinity of the outfall, as well as the coral reef. In support of this effort, in December 1990, a high-resolution sidescan-sonar and seismic-reflection survey was conducted over the area that could be affected by the sewage discharge using the research vessel *JEAN A* (owned and operated by the Commonwealth of Puerto Rico Department of Natural Resources) in order to provide a geologic framework, or basemap for the offshore component of this program. In this report, we present the sidescan-sonar imagery, the bathymetry of the study area, ship tracklines, sediment sample locations, grain size analyses of the sediment samples, and preliminary interpretation of the data set.

METHODS

The sidescan-sonar survey was conducted using a Klein 100 kHz system; total swath

width per trackline was 200 m. The sidescan data were logged digitally using a QMIPS data acquisition system (Danforth and others, 1991) at a sampling rate that resulted in a 0.1 m pixel size in the across track direction. Following the cruise, the data were decimated to a 0.4 m pixel size using a median filtering routine developed by Malinverno and others (1990) and were processed and mosaicked using procedures developed by Danforth and others (1991). This mosaic was then used as a basemap for the subsequent sampling phase of the investigation (Plate 1). Lighter tones on the sidescan-sonar images represent areas of relatively low acoustic backscatter intensity and darker tones, areas of high backscatter. Both the raw and processed sidescan data files are stored at the U.S. Geological Survey (USGS), Branch of Atlantic Marine Geology, Woods Hole, Massachusetts 02543.

Concurrent with the acquisition of the sidescan-sonar imagery, approximately 89 km of 3.5 kHz and Huntex Uniboom seismic-reflection profiles were collected. These data were recorded using an analog Raytheon recorder. The original profiles are also stored at the USGS, Woods Hole, Massachusetts. Ship tracklines that cover the study area and bathymetry derived from analysis of the 3.5 kHz profiles are presented on Plate 2. An additional series of 3.5 kHz and Uniboom seismic-reflection profiles were conducted southeast of the study area in an attempt to locate active faults and will not be discussed in this report; ship tracklines for these profiles are presented on Figure 2.

Bottom sediment samples were obtained in the study area using a Shipek grab sampler (see Plate 2 for sample locations; samples collected at stations B1 through B8 [five samples collected at each station; A through E] were used for biologic analysis). Grain-size analysis of the samples was conducted using a Coulter Counter following the methodology of Poppe and others (1985). Results of this textural analysis are presented in Tables 1 (sediment type is described using the class limits of Shepard, 1954) and 2 and textural statistics are presented in Table 3.

Ship navigation was conducted using a shorebase Miniranger transponder navigation system. Using these navigation data, the seismic-reflection profiles and bottom sample locations are accurate to within 5 m. The sidescan towfish, however, was not navigated independently of the ship, thus, an additional error of up to 15 m exists along-track in the sidescan imagery (Plate 1).

GEOLOGIC FRAMEWORK OF THE STUDY AREA

A sidescan-sonar mosaic is an approximate model of the interaction of sound with the sea floor that uses a two-dimensional display of pixels, each with an associated backscattering intensity. The level of backscattering is a function of, among other things (Reed and Hussong, 1989 and references therein), the sea-floor topography, roughness, and composition.

The Manchas Interiores-Manchas Exteriores reef complex is represented on the sidescan mosaic as an area of relatively high backscatter intensity (darker shades of gray) (Fig. 3). Areas of relatively low backscatter intensity (lighter shades of gray) within the reef complex represent either acoustic shadows or areas where the reef is covered by a thin veneer of sediment (Fig. 3). The reef complex is built on a regional Pleistocene (?) unconformity that is displayed on the seismic-reflection profiles (Fig. 4).

Sediment samples collected east (inshore) of the reef complex are dominantly clayey silt and silty clay (Plate 2 and Table 1). This sedimentary deposit is represented on the sidescan mosaic as an area of relatively low backscatter intensity (Fig. 3). High backscatter "blotches" on the sidescan mosaic are due to a large amount of biologic (?)

debris in the water column; probably related to the plume of suspended sediment originating from the Rio Grande de Anasco. This suspended sediment plume encroached on the reef complex during this survey. The muddy sedimentary deposit east of the reef complex, thought to be derived primarily from the Rio Grande Anasco, which blankets a Pleistocene (?) unconformity and thins from approximately 30 m thick in the northeastern part of the study area near the mouth of the Rio Grande Anasco to less than 8 m thick over an arch in the unconformity at latitude 18°14.5'N. and 18°14.0'N. (Fig. 5). In the extreme northeast segment of the sidescan-sonar mosaic (closest to the mouth of the Rio Grande Anasco), an area of relatively low backscatter intensity is interrupted by blotchy high-backscatter returns. These high backscatter returns are from material in the water column (Fig. 3). Seismic-reflection profiles collected over this area show evidence of gas-charged sediment; blanking of internal reflectors on the seismic-reflection profiles. Thus, the acoustic "noise" from the water column displayed on the sidescan imagery off the mouth of the Rio Grande de Anasco may be partly due to degassing of sediment, which common in other deltaic settings (Coleman and others, 1982).

The remaining sediment type, sandy reefal-derived sediment, was sampled off the northeast and northwest margin of the reef complex and within channels that run through the reef and typically has a relatively higher backscatter intensity than the muddy sedimentary deposit. Along the northeast margin of the reef complex a poorly developed moat has formed, probably in response to storm induced water flow (Plate 2 and Fig. 3). A minor moat may also exist along the southern margin of the reef complex (Plate 2 and Fig. 4). One gravelly sand sample, GS28, was rather unusual in that it was composed of a mixture of reefal and terrigenous material. These sandy deposits are suggested to be lag deposits that are formed by storm-surge-induced currents which flow through the channels in and around the margins of the reef complex.

Although no clear evidence of active faulting was observed on the seismic-reflection profiles (faults offsetting the sea floor), the trend of the northeastern margin of the reef complex is approximately N65°W, which is subparallel to the major structural lineaments observed in the adjacent onshore areas (Case and others, 1984). Thus, the morphological development of the reef complex may have been controlled by the local basement structure.

REFERENCES

- Case, J.E., Holcombe, T.L., and Martin, P.G., 1984, Map of geologic provinces in the Caribbean region: Geological Society of America Memoir 162, p. 1-30.
- Coleman, J.M., Prior, D.B., and Garrison, L.E., 1982, Subaqueous sediment instabilities in the offshore Mississippi River Delta: Environmental Information On Hurricanes, Deep Water Technology, and Mississippi Delta Mudslides In The Gulf of Mexico, Bureau of Land Management, Open File Report 80-02, p. 1-49.
- Danforth, W.W., O'Brien, T.F., and Schwab, W.C., 1991, USGS Image processing system: near real-time mosaicking of high-resolution sidescan-sonar data: Sea Technology, Jan. 1991, p. 54-59.
- Malinverno, A., Edwards, M., and Ryan, W.B.F., 1990, Processing of SeaMARC swath sonar data: IEEE Journal of Oceanic Engineering. vol. 15, p. 14-23.
- Poppe, L.J., Eliason, A.H., and Fredericks, J.J., 1985, APSAS - An automated particle size analysis system: U.S. Geological Survey Circular 963, 77 p.
- Reed, T.B., and Hussong, D., 1989, Digital image processing techniques for enhancement and classification of SeaMARC II side scan sonar imagery: Journal of Geophysical

Research, vol. 94, p. 7469-7490.
Shepard, F.P., 1954, Nomenclature based on sand-silt-clay ratios: *Journal of Sedimentary Petrology*: vol. 24, p. 151-158.

FIGURE CAPTIONS

- Figure 1. Location map of the study area.
- Figure 2. Map showing ship tracklines used to collect seismic-reflection profiles (3.5 kHz and Uniboom) south of the study area.
- Figure 3. General geologic interpretation of the sidescan-sonar imagery (Plate 1).
- Figure 4. Representative 3.5 kHz and Uniboom seismic-reflection profiles collected over the reef complex (A) and interpretive sketch (B) (Profile 13; see Plate 2 for the location).
- Figure 5. Representative 3.5 kHz and Uniboom seismic-reflection profiles collected across the muddy sedimentary deposit northeast of the reef complex (A) and interpretive sketch (B) (Profile 28; see Plate 2 for the location).

PLATE CAPTIONS

- Plate 1. SIDE-SCAN SONAR MOSAIC OF THE STUDY AREA
- Plate 2. SHIP TRACKLINES, SEDIMENT SAMPLE LOCATIONS, AND BATHYMETRY OF THE STUDY AREA

Table 1: General Textural Parameters

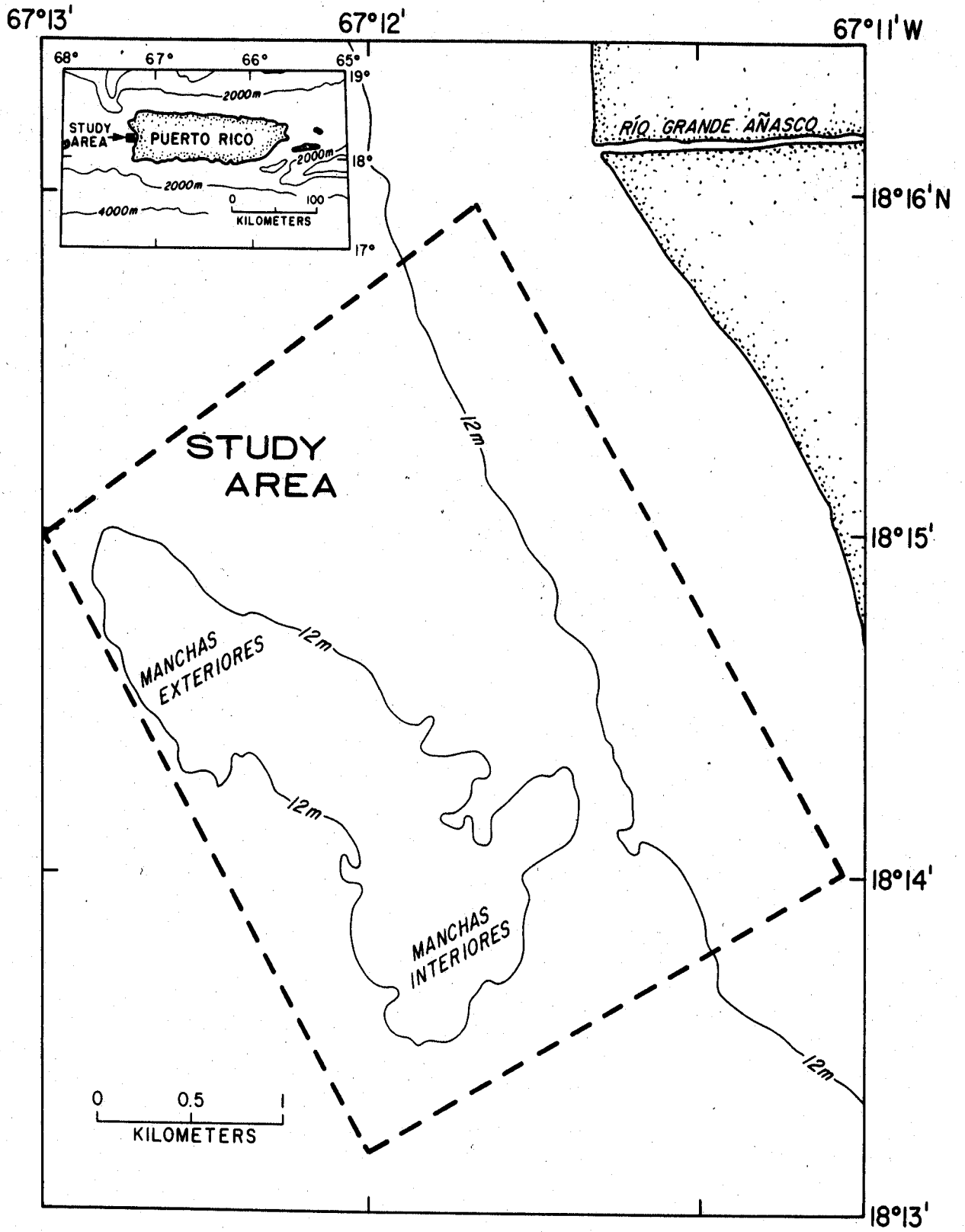
Sample	Gravel	Sand (%)	Silt (%)	Clay (%)	Sediment Type
GS01	0.00	0.11	49.06	50.84	SILTY CLAY
GS02	0.00	0.93	74.42	24.65	CLAYEY SILT
GS03	0.00	8.45	35.25	56.30	SILTY CLAY
GS04	0.13	0.62	36.52	62.73	SILTY CLAY
GS05	1.93	76.00	12.31	9.76	SAND
GS06	0.77	0.80	46.03	52.40	SILTY CLAY
GS07	1.60	2.80	38.48	57.12	SILTY CLAY
GS08	0.22	13.04	34.55	52.19	SILTY CLAY
GS09					NORECOVERY
GS10	0.74	5.51	47.51	46.25	CLAYEY SILT
GS11	0.42	13.89	44.91	40.77	CLAYEY SILT
GS12	0.04	4.60	58.14	37.22	CLAYEY SILT
GS13	0.00	2.15	48.24	49.60	SILTY CLAY
GS14					NORECOVERY
GS15	1.62	32.62	44.57	21.19	SANDY SILTY CLAY
GS16	2.34	35.97	37.08	24.61	SANDY SILTY CLAY
GS17	49.64	46.29	1.57	2.51	SANDY GRAVEL
GS18	0.44	27.97	49.16	22.43	SANDY SILTY CLAY
GS19	3.63	0.97	64.94	30.46	CLAYEY SILT
GS20	0.38	1.55	65.06	33.01	CLAYEY SILT
GS21	0.11	1.12	57.76	41.01	CLAYEY SILT
GS22	0.06	1.09	63.88	34.97	CLAYEY SILT
GS23	0.60	3.71	64.20	31.49	CLAYEY SILT
GS24	0.37	37.64	48.51	13.47	SANDY SILT
GS25	0.79	37.74	49.46	12.02	SANDY SILT
GS26	1.90	37.65	37.65	22.79	SANDY SILTY CLAY
GS27	2.21	51.74	37.43	8.63	SILTY SAND
GS28	11.72	83.59	2.55	2.15	GRAVELLY SAND
GS29	2.99	88.71	5.61	2.69	SAND
GS30	5.57	87.20	3.55	3.69	SAND
GS31	1.08	68.32	19.56	11.04	SILTY SAND
GS32	10.52	58.73	15.98	14.77	GRAVELLY SAND
GS33	10.34	86.80	1.59	1.28	GRAVELLY SAND

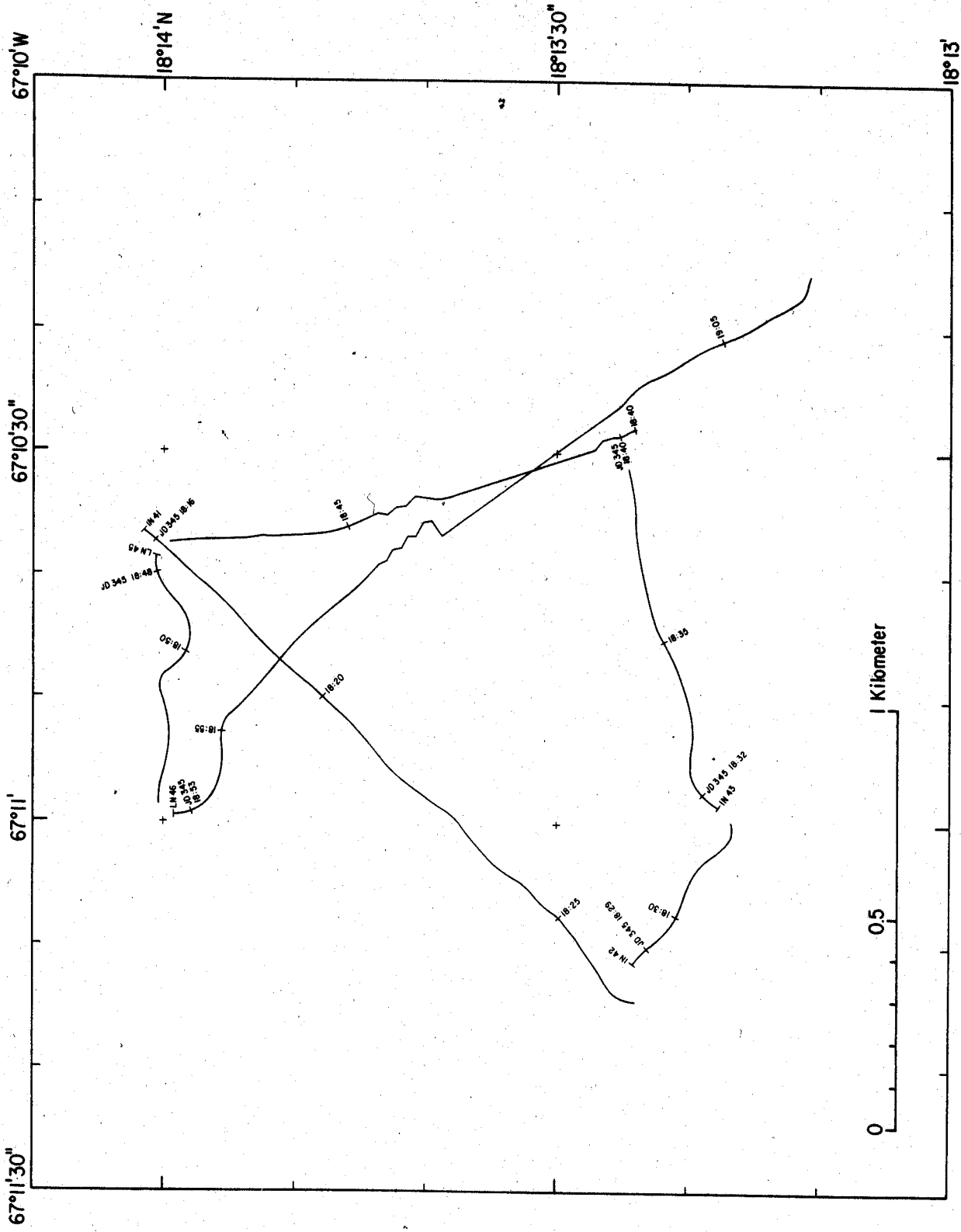
Table 2: Cumulative frequency percentage in Phi-size class.

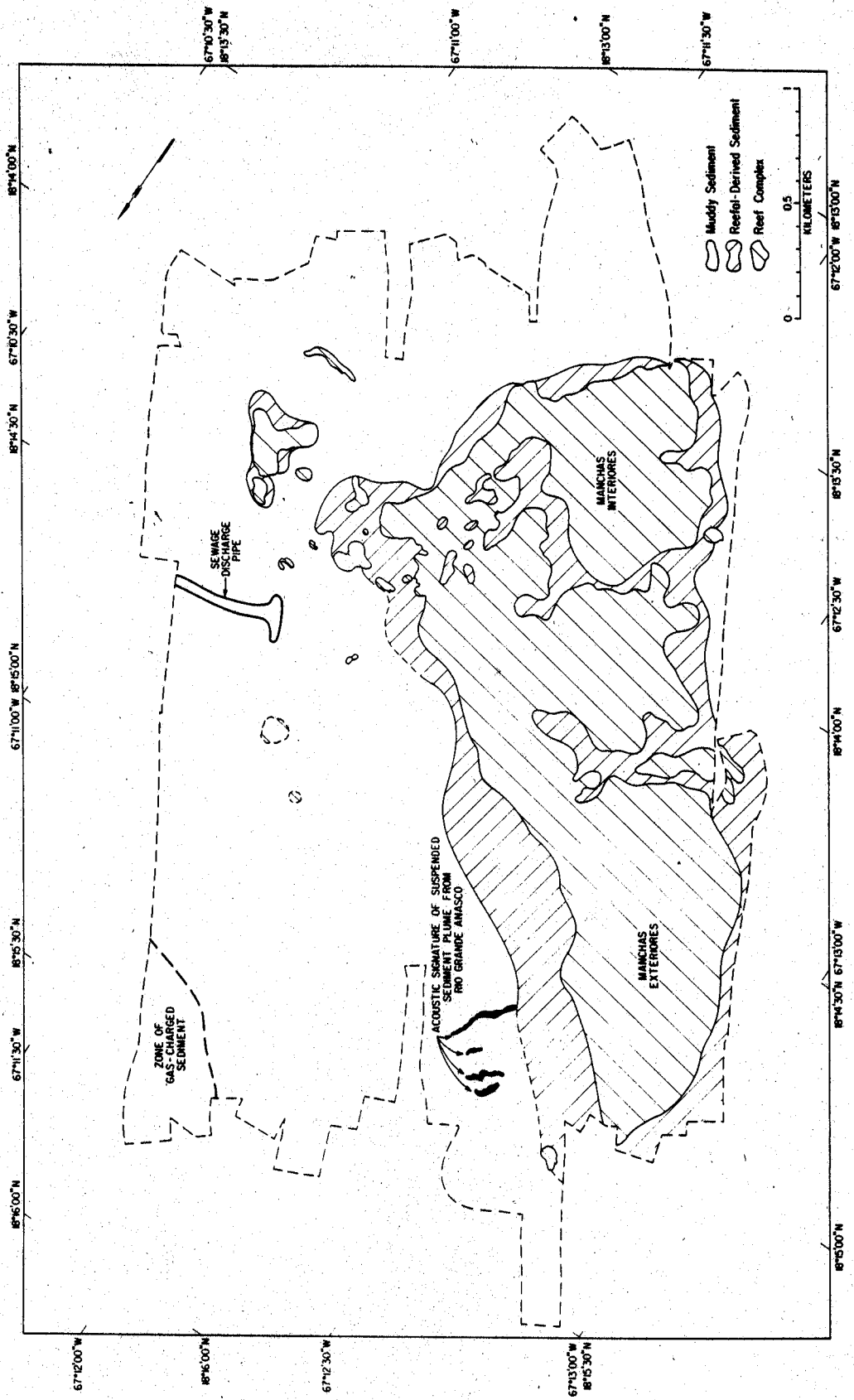
Sample	PH 11	PH 10	PH 9	PH 8	PH 7	PH 6	PH 5	PH 4	PH 3	PH 2	PH 1	PH -1	PH -2	PH -3	PH -4	PH -5
G801	100.00	90.05	69.27	49.16	31.21	13.24	2.03	0.11	0.00	0.00	0.00	0.00	0.00	0.00	0.00	0.00
G802	100.00	95.83	85.87	75.35	67.26	49.53	14.83	0.93	0.49	0.39	0.32	0.00	0.00	0.00	0.00	0.00
G803	100.00	99.38	84.97	43.70	29.33	18.32	9.78	8.45	4.97	2.01	0.82	0.00	0.00	0.00	0.00	0.00
G804	100.00	87.24	60.89	37.27	23.03	10.60	3.78	0.75	0.39	0.32	0.25	0.13	0.00	0.00	0.00	0.00
G805	100.00	98.08	94.08	90.24	87.27	84.88	81.60	77.93	70.06	44.87	19.81	1.93	0.00	0.00	0.00	0.00
G806	100.00	89.70	67.11	47.60	34.31	19.50	5.05	1.57	1.21	1.11	1.03	0.77	0.68	0.00	0.00	0.00
G807	100.00	89.41	65.52	42.88	27.55	13.40	5.86	4.40	3.16	2.55	2.16	1.60	0.00	0.00	0.00	0.00
G808	100.00	90.30	68.45	47.81	33.82	20.48	14.38	13.26	7.93	2.41	0.80	0.22	0.00	0.00	0.00	0.00
G809	100.00	91.47	72.39	53.75	41.70	29.77	17.06	6.24	2.70	1.37	1.13	0.74	0.00	0.00	0.00	0.00
G810	100.00	92.26	75.51	59.23	48.39	35.89	24.48	14.32	4.35	2.02	1.35	0.42	0.00	0.00	0.00	0.00
G811	100.00	93.55	78.48	62.78	44.08	23.01	8.10	4.84	1.52	0.55	0.39	0.04	0.00	0.00	0.00	0.00
G812	100.00	91.89	70.66	50.40	36.82	18.48	5.49	2.15	0.84	0.38	0.24	0.00	0.00	0.00	0.00	0.00
G813	100.00	95.74	86.96	78.80	72.02	63.00	49.56	34.23	7.43	3.95	2.95	1.82	0.00	0.00	0.00	0.00
G814	100.00	95.31	84.85	75.39	69.65	62.64	51.98	38.31	9.58	5.16	3.84	2.34	0.00	0.00	0.00	0.00
G815	100.00	99.57	96.51	97.49	96.71	96.29	96.08	95.92	95.29	89.20	72.28	49.64	45.04	38.50	24.86	0.00
G816	100.00	95.94	86.56	77.57	71.38	62.85	51.52	28.41	5.78	2.50	1.84	0.44	0.00	0.00	0.00	0.00
G817	100.00	95.73	84.29	69.54	50.04	27.50	10.61	4.60	4.28	4.21	4.12	3.63	0.00	0.00	0.00	0.00
G818	100.00	95.86	83.62	68.99	47.28	27.08	8.43	1.93	0.86	0.71	0.61	0.38	0.00	0.00	0.00	0.00
G819	100.00	94.11	78.53	58.99	38.71	18.89	4.46	1.23	0.85	0.64	0.42	0.11	0.00	0.00	0.00	0.00
G820	100.00	93.88	80.46	65.03	51.01	35.91	18.50	1.15	0.38	0.28	0.22	0.06	0.00	0.00	0.00	0.00
G821	100.00	94.72	82.33	68.51	55.38	42.59	24.44	4.31	1.57	1.20	1.05	0.60	0.00	0.00	0.00	0.00
G822	100.00	97.38	91.68	86.53	82.69	79.84	68.53	38.01	16.82	7.10	3.28	0.37	0.00	0.00	0.00	0.00
G823	100.00	98.06	93.31	87.98	82.70	77.16	60.94	38.53	18.36	6.74	3.54	0.79	0.00	0.00	0.00	0.00
G824	100.00	94.55	85.59	77.21	70.79	62.70	50.19	39.56	19.93	7.05	4.35	1.90	0.00	0.00	0.00	0.00
G825	100.00	98.29	94.72	91.37	88.84	86.79	79.07	53.95	27.83	9.50	5.18	2.21	0.00	0.00	0.00	0.00
G826	100.00	99.59	98.68	97.85	97.38	97.06	96.35	95.31	93.32	86.78	66.27	11.72	1.74	0.00	0.00	0.00
G827	100.00	99.43	98.29	97.32	96.74	95.99	94.26	91.72	74.32	39.20	19.86	2.99	1.06	0.00	0.00	0.00
G828	100.01	99.32	97.67	96.32	95.54	95.00	94.01	92.77	86.65	71.23	45.31	5.57	0.00	0.00	0.00	0.00
G829	100.00	98.20	93.74	88.96	84.91	81.17	74.48	69.41	39.58	26.38	14.63	1.08	0.00	0.00	0.00	0.00
G830	100.00	91.23	85.23	80.98	80.98	77.20	72.16	69.25	62.54	48.84	34.19	10.52	3.37	0.00	0.00	0.00
G831	100.00	99.81	99.29	98.74	98.26	97.89	97.55	97.16	96.53	81.44	39.55	10.34	4.77	2.73	0.00	0.00
G832	100.03	99.81	99.29	98.74	98.26	97.89	97.55	97.16	96.53	81.44	39.55	10.34	4.77	2.73	0.00	0.00
G833	100.03	99.81	99.29	98.74	98.26	97.89	97.55	97.16	96.53	81.44	39.55	10.34	4.77	2.73	0.00	0.00

Table 3: Inclusive graphical statistics of textural data in phi-units

Sample	Median GS	Mean GS	Stan. Dev.	.Skewness	Kurtosis
GS01	8.04	7.95	1.57	-0.08	-0.99
GS02	6.03	6.59	1.76	0.25	-0.06
GS03	8.30	7.80	2.14	-0.58	1.08
GS04	8.54	8.25	1.65	-0.49	1.71
GS05	2.20	2.93	2.73	0.61	0.76
GS06	8.12	7.79	1.98	-0.66	4.25
GS07	8.31	7.90	2.14	-0.93	5.23
GS08	8.11	7.50	2.38	-0.52	0.49
GS09					
GS10	7.69	7.31	2.24	-0.38	0.69
GS11	7.15	6.91	2.42	-0.25	-0.31
GS12	7.32	7.32	1.83	-0.23	0.50
GS13	7.97	7.73	1.78	-0.26	0.10
GS14					
GS15	5.03	5.52	2.52	0.06	-0.18
GS16	4.85	5.48	2.72	0.03	-0.39
GS17	-0.96	-1.05	3.13	0.48	1.25
GS18	4.93	5.64	2.40	0.16	-0.44
GS19	7.00	6.87	2.30	-0.82	4.37
GS20	7.14	7.16	1.75	-0.26	1.70
GS21	7.56	7.53	1.67	-0.28	1.39
GS22	6.93	7.03	1.91	0.01	-0.72
GS23	6.58	6.72	2.10	-0.13	0.37
GS24	4.39	4.76	2.30	0.32	0.42
GS25	4.51	4.80	2.29	0.19	0.29
GS26	4.98	5.33	2.82	0.04	-0.61
GS27	3.85	4.09	2.22	0.33	1.39
GS28	0.49	0.73	1.91	1.14	7.85
GS29	2.31	2.31	1.88	0.61	4.39
GS30	1.18	1.53	2.13	0.98	5.04
GS31	3.35	3.72	2.69	0.34	-0.05
GS32	2.08	2.95	3.54	0.30	-0.74
GS33	1.25	1.08	1.76	0.48	6.48







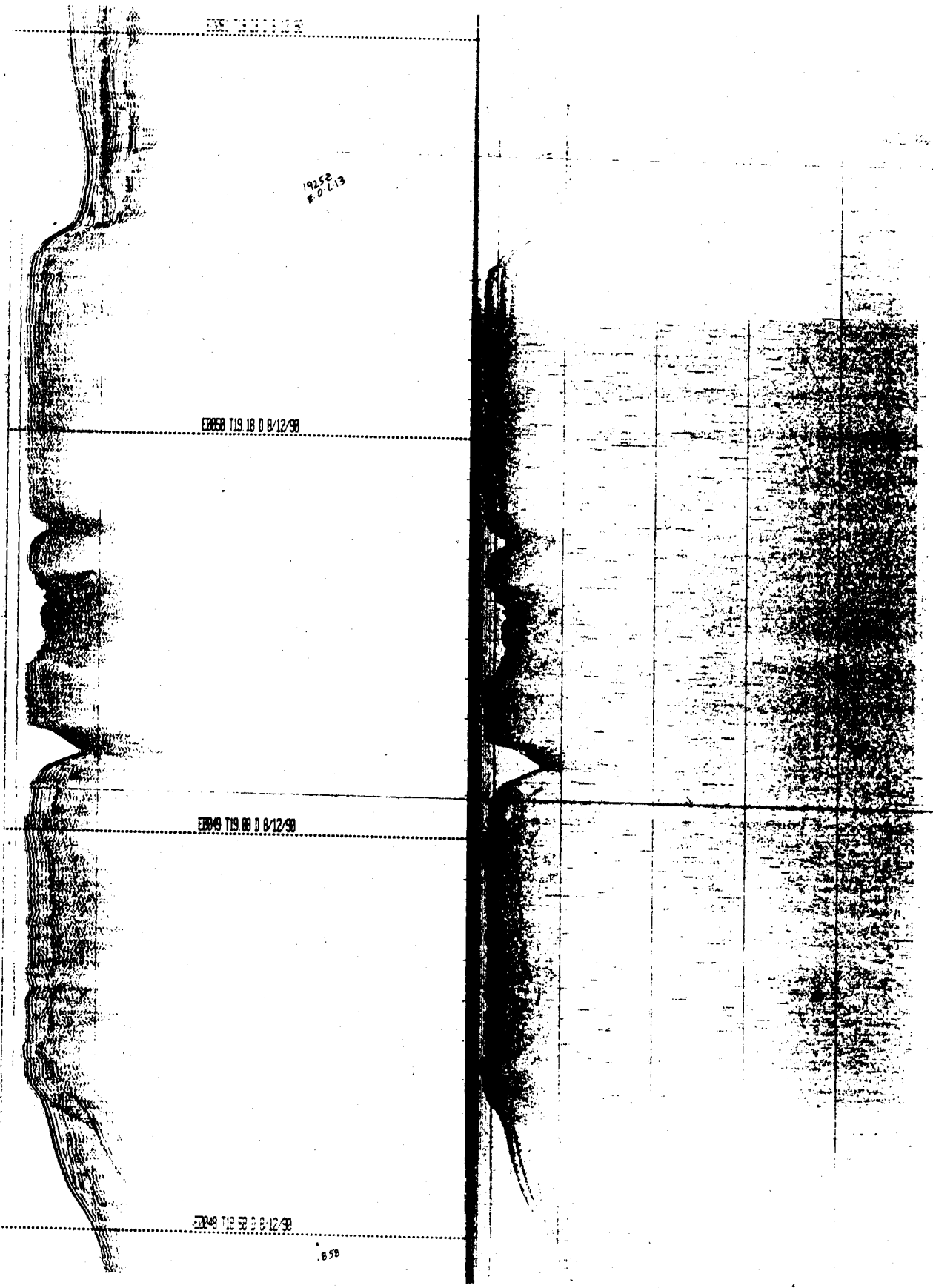


FIGURE 4A.

19252
8.07.13

E0049 719 00 0 0/12/90

E0049 719 00 0 0/12/90

E0049 719 00 0 0/12/90

858

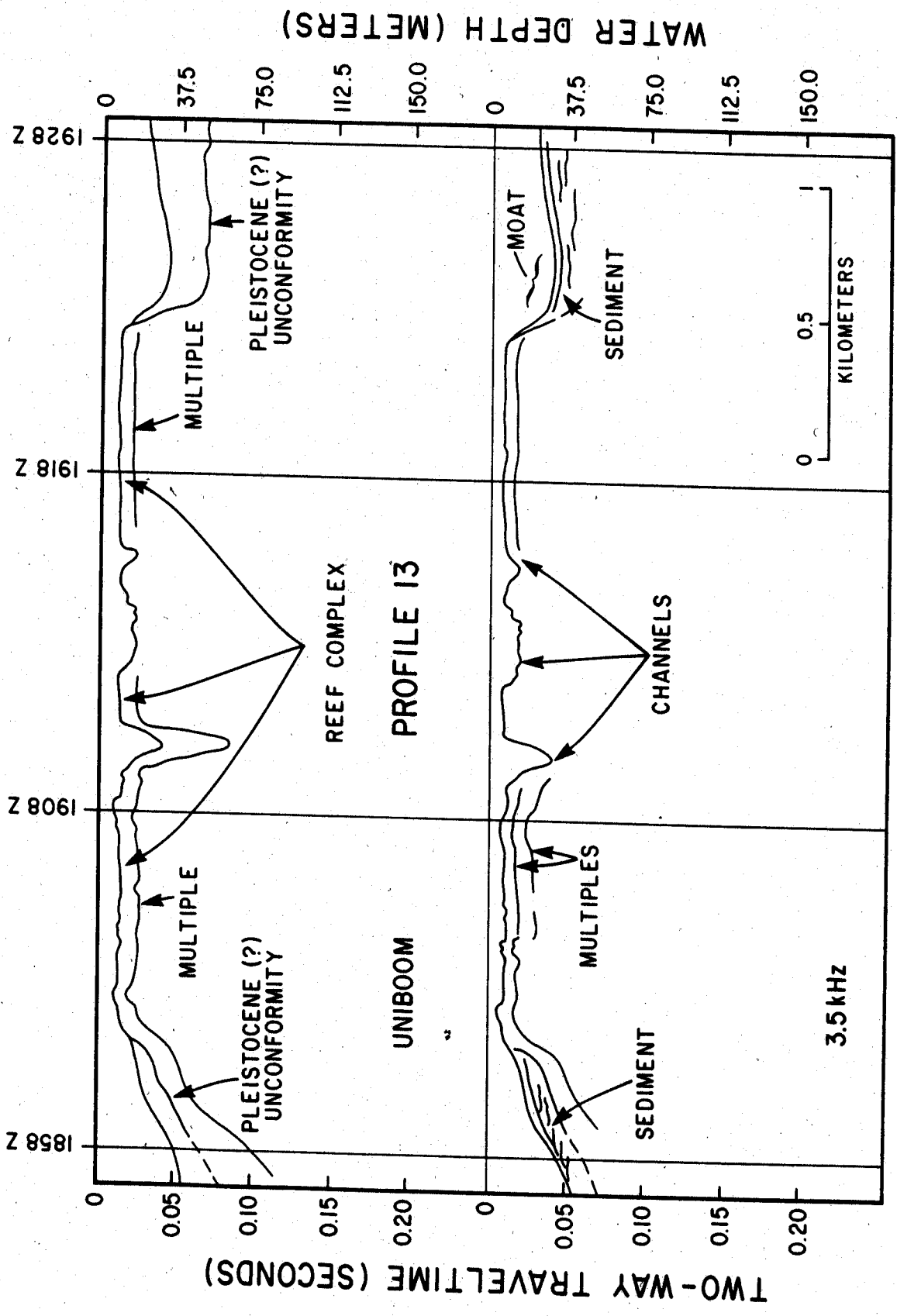


FIGURE 4B.

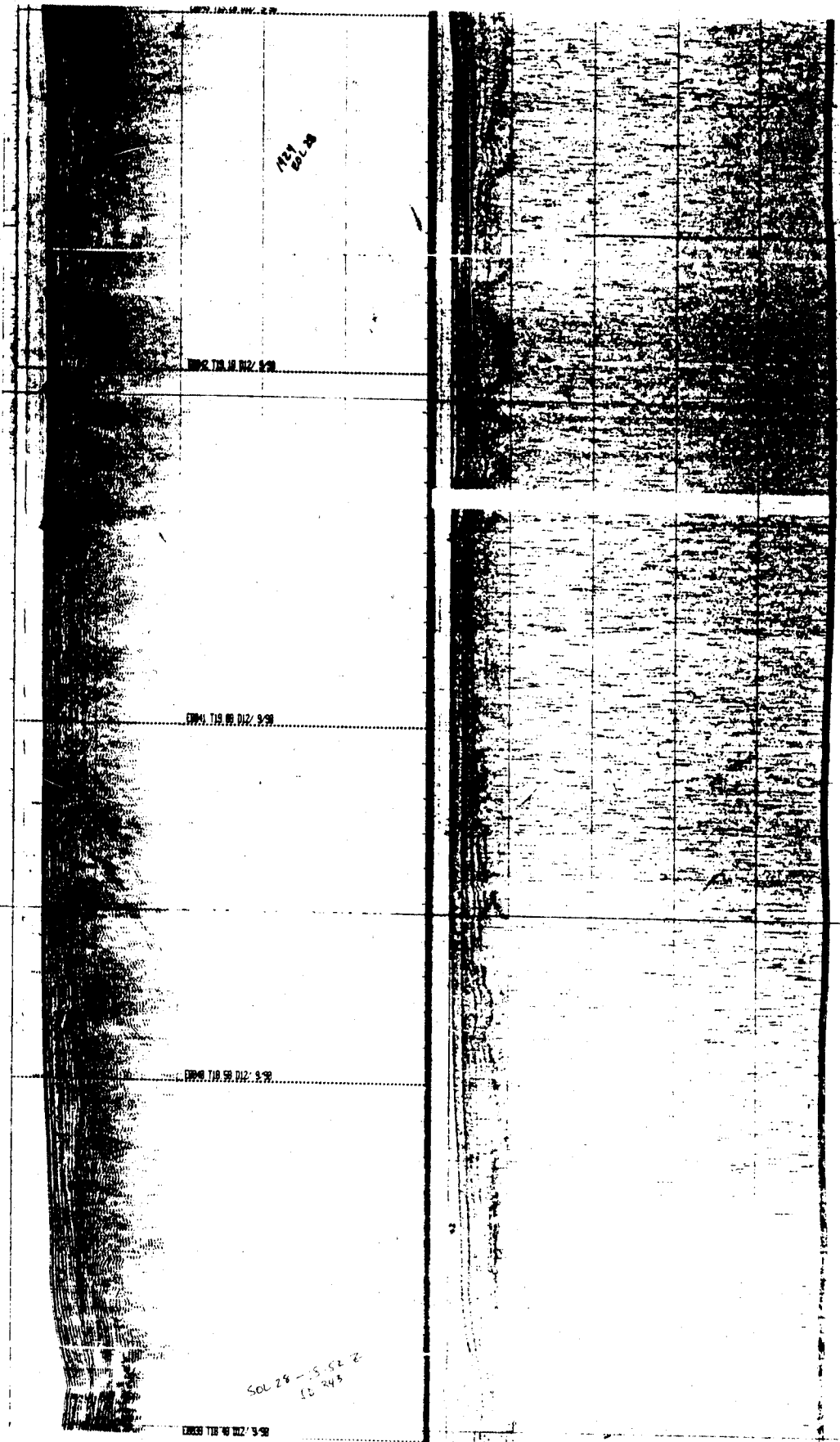


FIGURE 5A.

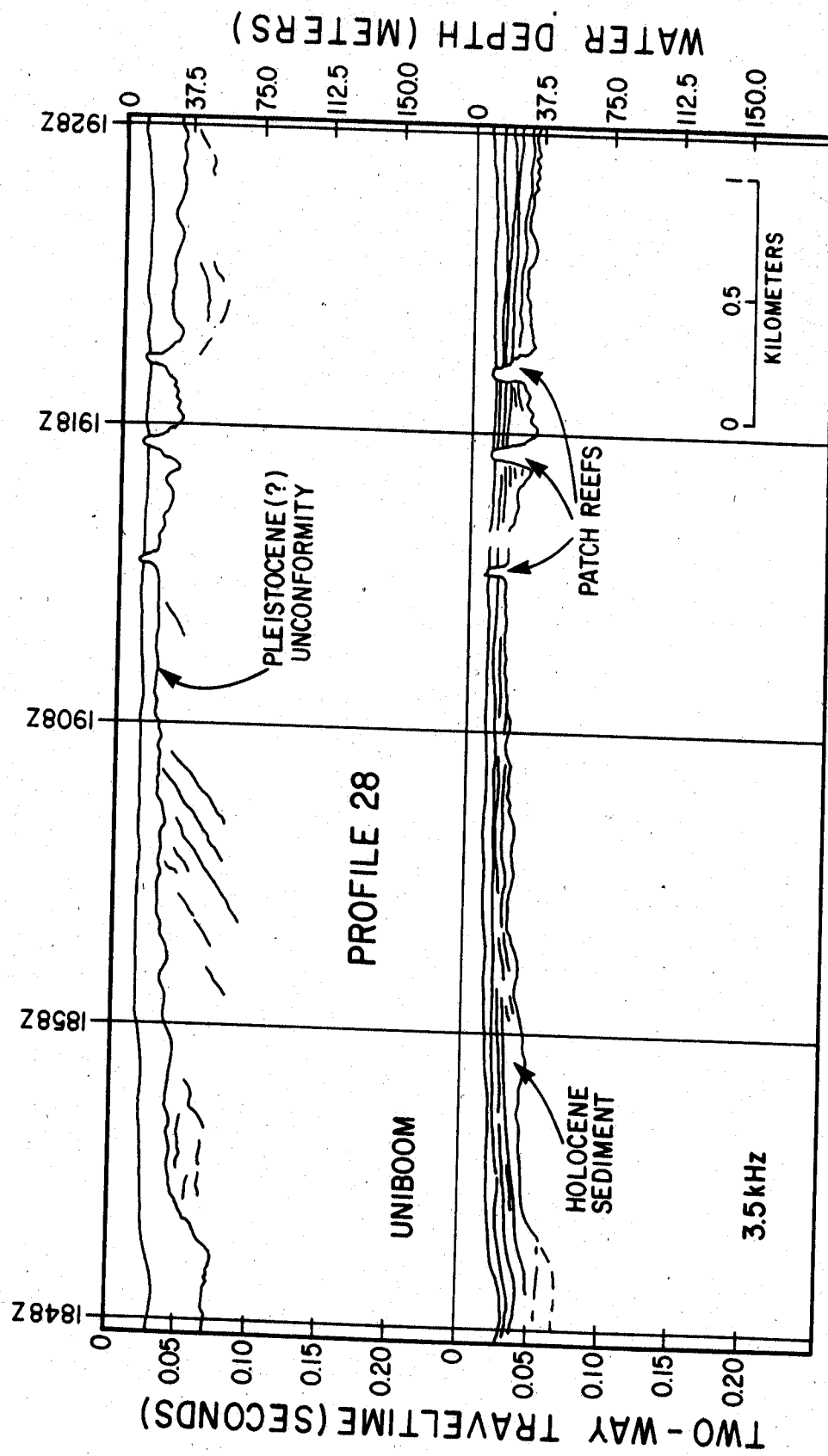


FIGURE 5B.